Strong Electron-Phonon Coupling Regime in Quantum Dots: Evidence for Everlasting Resonant Polarons

S. Hameau, Y. Guldner, O. Verzelen, R. Ferreira, and G. Bastard
Laboratoire de Physique de la Matière Condensée, Ecole Normale Supérieure, 24 rue Lhomond, 75231 Paris Cedex 05, France

J. Zeman
Grenoble High Magnetic Field Laboratory, CNRS/MPI, 25 avenue des Martyrs, 38042 Grenoble Cedex 9, France

A. Lemaître and J. M. Gérard
France Telecom/CNET/DTD/CDP, BP 107, 92225 Bagneux Cedex, France
(Received 22 April 1999)

Using far-infrared magnetospectroscopy in self-assembled InAs quantum dots, we have investigated the electronic transitions from the ground s levels to the excited p levels. The experiments consist of monitoring, by means of Zeeman tuning of the excited level, a resonant interaction between the discrete ($p, 0$ LO phonon) state and the continuum of either ($s, 1$ LO phonon) or ($s, 2$ LO phonons). We show that the electrons and the LO phonons are always in a strong coupling regime and form an everlasting mixed electron-phonon mode.

PACS numbers: 73.40.Kp, 73.20.Dx, 78.20.Ls

Electrons in excited atomic states can relax towards lower lying levels by spontaneous emission of photons. Artificial atoms like semiconductor quantum dots display discrete levels. For electrons (or holes) placed in excited levels the spontaneous emission of photons is inefficient for the relaxation due to the characteristic energy splitting of the dot states (~50 meV in a ~20 nm dot). The carriers bound to these artificial atoms are however in interaction with phonons which display a continuum of finite width, unlike photons. It has been shown that the intradot relaxation through acoustical phonons is totally inefficient, the energy mismatch between electron states being much too large [1,2]. In semiconductors, the most powerful energy relaxation channel is (by far) the irreversible emission of longitudinal optical (LO) phonons through the Fröhlich coupling. Despite its effectiveness, this electron-phonon coupling is weak, to the extent that the initial discrete level ($e, 0$ phonon) irreversibly decays into the continuum ($g, 1$ phonon) where e and g, respectively, denote an excited state and the ground electronic state. Such a weak coupling is very well described by the Fermi golden rule in bulk, quantum well (2D) or quantum wire (1D) structures. Because the optical phonons show very little dispersion, it has been argued that the LO phonon assisted relaxation in semiconductor quantum dots could be efficient only if the energy separation between the electronic states differs by one (or several) LO phonons. Here we present experimental evidence supported by theoretical modeling that the very idea of an electron emitting LO phonons and relaxing irreversibly to a less excited state (as in bulk, 2D, and 1D heterolayers) is wrong in a quantum dot. What happens in reality is that the electrons and the LO phonons are in a strong coupling regime and form everlasting mixed electron-phonon modes, as recently suggested by Inoshita and Sakaki in the case of one phonon [3]. Using far-infrared (FIR) magnetospectroscopy, we have investigated the $g \rightarrow e$ transition in self-assembled doped InAs quantum dots. The experiments consist of monitoring, by means of Zeeman tuning of the dot excited level e, a resonant interaction between the discrete ($e, 0$ LO phonon) state and the continuum of either ($g, 1$ LO phonon) or ($g, 2$ LO phonons). We show that the ($e, 0$ LO phonon) state does not dissolve when entering into the continuum but forms a hybrid mode with ($g, 1$, or 2 LO phonons).

The growth parameters of the self-assembled InAs quantum dots (QDs) sample have been chosen in order to strengthen the resonant FIR absorption. Our sample was grown on a (001) GaAs substrate by molecular beam epitaxy using the Stranski-Krastanov growth mode of InAs on GaAs [4]. It consists of 30 layers of InAs QDs separated by 50 nm GaAs barriers. The density of QDs is $\sim 4.10^{10}$ cm^{-2} for each InAs layer, corresponding to an average center to center distance of 50 nm, which is enough to neglect the interactions between dots. The delta-doping level of each GaAs barrier ($\sim 8 \times 10^{10}$ cm^{-2}) was adjusted in order to transfer on average one electron per dot and to populate only their lowest states. The shape of the InAs QDs, estimated from transmission electron micrographs, is lenslike with a typical height of ~2 nm and a lateral diameter around 20 nm. The gap of the dot measured from photoluminescence experiments is 1.17 eV at 77 K.

Because of the quasicylindrical symmetry of the InAs QDs, the ground and first excited states of the dots are s-like and p-like, respectively. The sample transmission $T(0)$ was recorded by Fourier-transform spectroscopy in the FIR range 100–700 cm^{-1} at 4 K. The s-p absorption

 0031-9007/99/83(20)/4152(4)$15.00

consists of two resonances: For radiation linearly polarized along the [110] direction, only the upper component is excited at 63 meV. On the contrary, only the lower one appears at 56.3 meV for polarization along $[1\bar{1}0]$. Both resonances are observed with comparable intensity for an intermediate polarization along [100] or for unpolarized radiation. The strong intensity of the FIR absorption (~9%) as well as the sharpness of the lines (the linewidth at half amplitude is ~4 meV) demonstrates the good homogeneity of this multilayered sample. The 6.7 meV splitting between the two components can be explained by the slight elongation of the InAs dots along the $[1\bar{1}0]$ direction [5]. Such an anisotropy in the growth plane mixes the p states to produce two split levels π_+ and π_- so that the two transitions s-π_+ and s-π_- can be excited depending on the polarization. Modelization (effective mass calculations) of the transition energies using a realistic shape for the QDs leads to a dot size of 19 nm along $[1\bar{1}0]$ and 17 nm along [110]. The deduced 10% anisotropy in the growth plane is found in good agreement with previously reported TEM observations [6].

FIR magnetotransmission was studied at 2 K up to 13 T using a superconducting solenoid and up to 23 T using a resistive magnet. The magnetic field B was applied perpendicular to the layers and the sample transmission $T(B)$ was normalized by the zero field spectrum $T(0)$ to eliminate the optical setup effects. Figure 1 displays the transmission ratio $T(B)/T(0)$ between 6 and 15 T. Both $T(B)$ and $T(0)$ are measured for unpolarized radiation. Two main transmission minima are observed whose energy splitting is found to increase with B because of the orbital Zeeman effect of the p states. The magnetic field dispersion of the resonances consists essentially in three branches, as shown in Fig. 2. Taking into account the Zeeman effect and the energy splitting δ at $B = 0$ between the π_- and π_+ states, a simple perturbation approach yields the following dispersion relation for the s-π_+ and s-π_- transitions:

$$E_\pm = E_0 \pm \frac{1}{2}\sqrt{(\hbar\omega_c)^2 + \delta^2}, \tag{1}$$

where E_0 is the average s-p energy separation at $B = 0$ and ω_c is the cyclotron frequency. The best fit to the $B = 0$ results leads to $E_0 = 60$ meV and $\delta = 6.8$ meV, whereas the fit to the B dispersion using Eq. (1) (shown by the dashed lines in Fig. 2) gives a cyclotron mass $m_c = 0.067 \pm 0.003 m_0$. Such an effective mass is consistent with the value obtained in previous FIR magneto-optical experiments [5]. It is clear in Fig. 2 that

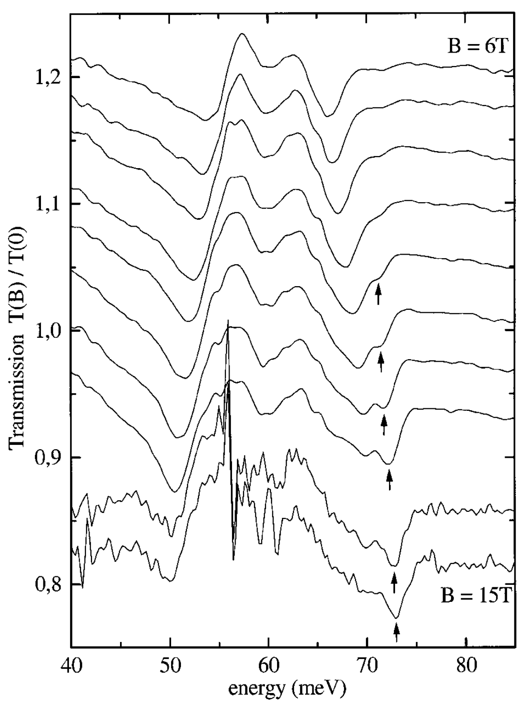

FIG. 1. Transmission ratio $T(B)/T(0)$ at $T = 2$ K for magnetic field B between 6 and 15 T. Traces have been offset for clarity. The additional resonance appearing at $B = 10$ T whose magnitude increases with B is shown by the arrows.

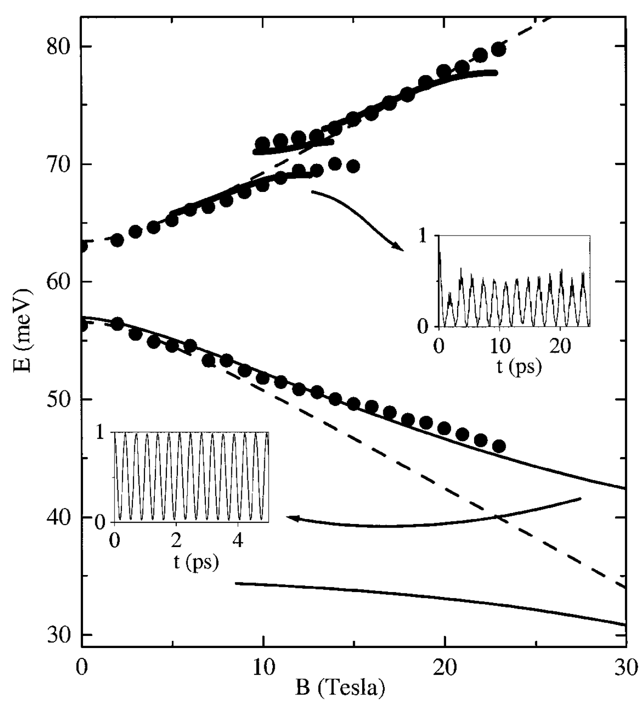

FIG. 2. Magnetic field dispersions of the resonances (full circles). The dashed lines are the calculated dispersions from Eq. (1). The bold solid lines show the calculated coupling between $|\pi_+, 0\rangle$ and $|s, 2\rangle$. The direct interactions between $|\pi_-, 1\rangle$ and $|s, 2\rangle$ redistributes the $|s, 2\rangle$ continuum into two ones and the indirect interactions of $|\pi_+, 0\rangle$ with the two splitted $|s, 2\rangle$ continua provokes two anticrossings, so that three lines separated by uneven gaps are calculated. Because of the inhomogeneous broadening, the smaller anticrossing is not observed in the experiments. The solid lines are the calculated anticrossing between $|\pi_-, 0\rangle$ and $|s, 1\rangle$. The time dependence of the survival probability in the $|\pi_+, 0\rangle$ ($|\pi_-, 0\rangle$) state at $B = 11$ T ($B = 28$ T) is shown in the upper (lower) inset.

striking anomalies occur in the experimental dispersions as compared to the predicted ones given by the dashed lines. First, an anticrossing is observed around 70 meV and 12 T. Second, the dispersion of the lowest branch considerably deviates from its expected behavior for $B \geq 8$ T. We argue now that these two effects result from the strong electron-LO phonon coupling regime in a totally confined system. Let us focus initially on the anticrossing at $\sim$70 meV. This value corresponds to about twice the energy $\hbar\omega_{\mathrm{LO}}$ of a LO phonon either in GaAs or in InAs strained to GaAs [7]. As shown by the arrows in Fig. 1, an additional absorption line appears at $B = 10$ T whose magnitude increases with B so that a doublet is clearly observed in the field range 10–15 T. This effect resembles the well-known anomalies observed in the dispersion of interband or intraband magneto-optical transitions towards the $n = 1$ conduction Landau level in bulk semiconductors. At the magnetic field for which the ($n = 0$, one LO phonon) Landau level becomes resonant with the ($n = 1$, no phonon) Landau level, an anticrossing is usually observed because of the resonant polaron interaction [8–10]. Here, since the observed anticrossing arises at roughly $2\hbar\omega_{\mathrm{LO}}$ above the ground s state, we naturally associate it to the coupling between mixed electron-lattice states differing by two LO phonons. Thus, the anticrossing occurs for magnetic field at which the (π_+ level, no phonon) becomes resonant with the (s level, two LO phonons). The coupling energy deduced from these data is about 2 meV, which is surprisingly large as it corresponds to the magnitude of the usual resonant polaron with *one* LO phonon in III-V bulk semiconductors [8,9].

In order to explain the origin and the magnitude of this anticrossing, we have calculated the coupling between the relevant mixed electron-lattice states. In the presence of phonons, the dot eigenvectors write in terms of the states $|x, n\rangle$, where x represents one electron level (s, π_+, $\pi_-, \ldots$) and n describes one state of the phonon system ($n = 0$ for pure electron levels; $n = 1$ for the manifold of states with one phonon, $n = 2$ for the two-phonon manifold, etc....). We shall thus focus below on the phonon-mediated coupling between the zero-phonon state $|\pi_+, 0\rangle$ and the manifold $|s, 2\rangle$ of two-phonon states (with the same or different wave vectors). Actually, in our numerical modeling we retain also the one-phonon manifold $|\pi_-, 1\rangle$. The reason to include $|\pi_-, 1\rangle$ in our basis is because it has come close to $|s, 2\rangle$ at the field where this later interacts with $|\pi_+, 0\rangle$. The electron-phonon interaction is described by the Fröhlich Hamiltonian which is linear in the phonon creation and annihilation operators and thus couples only states differing by one optical phonon. This means that there is no direct coupling between the $|\pi_+, 0\rangle$ and $|s, 2\rangle$ states. They are nevertheless both coupled to the $|\pi_-, 1\rangle$ states. In addition, second-order couplings exist between the basis states, which correspond to virtual excursion processes to states pertaining to different phonon manifolds. Finally, diagonal corrections also appear, which renormalize the energies of the basis states. Figure 3 presents the levels of interest for the calculations: The full lines are for the basis states and the dashed lines (apart the $|s, 0\rangle$ one) for the states contributing to the second-order processes. LO phonons were taken bulklike. This is not unreasonable to the extent that the dots are relatively big and involve thousands of units cells. We have neglected the finite lifetime of the LO phonons. To comply with the experiments we took the energy of the zone center phonons to be equal to 36 meV and a Fröhlich coupling constant $\alpha = 0.15$, significantly larger than in bulk GaAs or InAs. The possibility of an enhanced α in InAs QDs was recently suggested by Heitz *et al.* [11] in order to interpret optical data and was also proposed in II-VI nanocrystals [12]. The LO phonon dispersion $\omega_{\mathrm{LO}}(q)$ was taken into account as follows. We took $N = 56$ values for the wave vector q close from the center of the Brillouin zone (we have checked that retaining $N = 80$ values leads to the same results). This is because the Fröhlich interaction favors small wave vectors as it varies in $1/q$. The largest q value was such that any matrix element for yet larger q values was less than 1% of its largest value. This reduces the effective energy width of the one and two phonon continua to about 0.4 and 0.8 meV, respectively.

The matrix diagonalization accounts for the direct and indirect couplings between the $|\pi_+, 0\rangle$, $|\pi_-, 1\rangle$, and $|s, 2\rangle$ basis states and produces a large number of eigenvalues, which represent physically quite different eigenstates Ψ_n $n = 1, \ldots, 1 + N + N(N + 1)/2$). The experiment (the magnetoabsorption due to the electric dipole allowed transition between the zero-phonon $|s, 0\rangle$ and $|\pi_+, 0\rangle$ states) provides information on the projection $P_n = \langle \Psi_n | \pi_+, 0\rangle$ of the full dot eigenstates on the $|\pi_+, 0\rangle$ state. To compare with experiments, the bold solid lines in Fig. 2 show

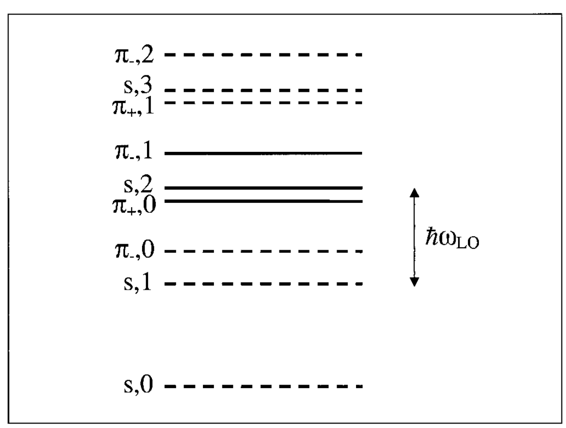

FIG. 3. Schematic representation (for a field near the two phonons resonance) of the electron/phonon levels leading to second-order corrections (dashed lines) when projected onto the Hamiltonian related to the basis states (full lines).

the B dependence of all the calculated eigenstates with projection $|P_n|^2 > 0.1$ (which is roughly the experimental sensitivity). There is good agreement between our modeling and the experiments. We note in particular that the overall magnitude of the anticrossing, about 2 meV, is well described by our modeling with bulk LO phonons. The salient feature of the experiments which is well explained by the theory is that the discrete state $|\pi_+, 0\rangle$ does not dissolve completely in the $|s, 2\rangle$ continuum but, to a large extent, keeps existing. For instance, we have obtained that the time dependence of the survival probability in the $|\pi_+, 0\rangle$ level $|P_n(t)|^2$ $[P_n(0) = 1]$ is definitely not exponential but displays everlasting oscillations which are shown in the upper inset of Fig. 2 for $B = 11$ T. We therefore conclude that the electron-two LO phonons interaction in quantum dots never shows a weak coupling behavior and can never be taken into account by means of the Fermi golden rule.

A still stronger anomaly is expected in the dispersion of the s-π_- transition when $|\pi_-, 0\rangle$ becomes resonant with the $|s, 1\rangle$ manifold (at magnetic field for which the s-π_- transition energy is around $\hbar\omega_{\mathrm{LO}} \approx 36$ meV). As shown in Fig. 2, this would happen around $B = 28$ T which is beyond our magnetic field range. Nevertheless, the strong departure of the lowest branch from the dashed line observed for $B \geq 8$ T shows the existence of a huge anticrossing between $|\pi_-, 0\rangle$ and $|s, 1\rangle$. The observed dispersion is actually what we calculate, as shown by the solid lines in Fig. 2. The plot versus B of all the levels (obtained very much as in the previous two-phonon case but spanned on a basis which is more appropriate for the one-phonon anticrossing) with squared projection on the $|\pi_-, 0\rangle$ level larger than 0.1 reveals an energy anticrossing of about 12 meV, 1 order of magnitude larger than that observed in bulk III-V semiconductor [8–10]. The calculated upper branch of this anticrossing is in very good agreement with the experimental dispersion. The time dependence of the survival probability in the $|\pi_-, 0\rangle$ level, shown in the lower inset in Fig. 2 for $B = 28$ T, is a Rabi oscillation. Even more so than in the two phonons case the coupling between electron and one-phonon continuum is strong and in no case can be treated perturbatively, as recently pointed out by Inoshita and Sakaki [3].

To summarize, we have investigated electronic transitions from the ground s state to the excited π_- or π_+ states in self-assembled InAs quantum dots. Using the Zeeman effect of the excited levels, we were able to monitor the resonant interaction between the discrete (π_- or $\pi_+, 0$ LO phonon) states and the continuum of either ($s, 1$ LO phonon) or ($s, 2$ LO phonons). The magnetic field dispersion of the transmission minima evidenced a $|\pi_+, 0\rangle$, $|s, 2\rangle$ anticrossing with the formation of a 2 LO-phonons polaron as well as a huge anticrossing between $|\pi_-, 0\rangle$ and $|s, 1\rangle$. In order to explain the origin and the magnitude of these anticrossings, we have calculated the coupling between the relevant mixed electron-lattice states from which we demonstrate that the electron-LO phonon interaction in quantum dots never shows a weak coupling behavior and can never be described by means of the Fermi golden rule. The strong coupling regime which is always observed with the formation of everlasting polarons is a novel type of electron-phonon behavior in heterostructure physics.

[1] U. Bockelmann and G. Bastard, Phys. Rev. B **42**, 8947 (1990).

[2] H. Benisty, C. M. Sottomayor-Torres, and C. Weisbuch, Phys. Rev. B **44**, 10 945 (1991).

[3] T. Inoshita and H. Sakaki, Phys. Rev. B **56**, R4355 (1997).

[4] L. Goldstein, F. Glas, J. Y. Marzin, M. N. Charasse, and G. Le Roux, Appl. Phys. Lett. **47**, 1099 (1985).

[5] M. Fricke, A. Lorke, J. P. Kotthaus, G. Medeiros-Ribeiro, and P. M. Petroff, Europhys. Lett. **36**, 197 (1996).

[6] Y. Nabetani, T. Ishikawa, S. Noda, and A. Sasaki, J. Appl. Phys. **76**, 347 (1994).

[7] P. D. Wang, N. N. Ledentsov, C. M. Sotomayor-Torres, I. N. Yassievich, A. Pakhomov, A. Yu. Egovov, P. S. Kop'ev, and V. M. Ustinov, Phys. Rev. B **50**, 1604 (1994).

[8] See, e.g., C. R. Pidgeon, in *Handbook on Semiconductors*, edited by M. Balkanski (North-Holland Publishing Company, Amsterdam, 1980), Vol. 2, p. 270, and references therein.

[9] E. J. Johnson and D. M. Larsen, Phys. Rev. Lett. **16**, 655 (1966).

[10] Y. J. Wang, H. A. Nickel, B. D. McCombe, F. M. Peeters, G. Q. Hai, J. M. Shi, J. T. Devreese, and X. G. Wu, in *High Magnetic Field in the Physics of Semiconductors II*, edited by G. Landwehr and W. Ossau (World Scientific Publishing Company, Singapore, 1997), Vol. 2, p. 797.

[11] R. Heitz, M. Veit, N. N. Ledentsov, A. Hoffmann, D. Bimberg, V. M. Ustinov, P. S. Kop'ev, and Zh. I. Alferov, Phys. Rev. B **56**, 10 435 (1997).

[12] G. Scamarcio, V. Spagnolo, G. Ventruti, M. Lugara, and G. C. Righini, Phys. Rev. B **53**, 10 489 (1996).